

The Effect of wing twist Distortion on Glider static longitudinal Stability with Stick fixed

By Tadeusz Labuc and Stanislaw Skrzydlewski, Szybowcowy Zaklad Doswiadczalny, Poland

Presented at the 10th OSTIV Congress, South Cerney (England), June 1965

Summary

The paper deals with static stability margin, with particular respect to the effects of elasticity, that is to the finite stiffness of the sailplane. The expression for static margin is derived on the basis that the distortion can be expressed simply as a change of incidence of the tailplane. Calculations for the Foka sailplane are compared with flight test measurements made by the trein-curve method, the distortion being measured photographically during the test. The distortion so measured was the one used in the calculations. At high C_L (low speed) the calculation and measurements differ a little, but in the low C_L (high speed) regime, in which distortion effects are large, the agreement is good.

1. Introduction

Recently at the Szybowcowy Zaklad Doswiadczalny the principle has been adopted that the static stability of prototype and series gliders shall be proved quantitatively over the whole range of speeds from the stall to the placard speed. The determination of static stick-fixed stability is based on the elevator deflection measurements, the control column movement not being of interest.

The results obtained in this way have shown significant differences when compared with calculations especially in the character of the variation of the static margin with lift coefficient. To explain these differences theoretical and experimental work has been performed; this paper gives the results of this investigation.

2. Symbols

- a - Glider lift curve slope $\delta C_L/\delta \alpha$
- a_1 - Tailplane lift curve slope $\delta C_{LT}/\delta \alpha_T$
- a_2 - $\delta C_{LT}/\delta \eta$
- b - Wing span
- c - Wing chord
- \bar{c} - Mean aerodynamic chord
- C_L - Wing lift coefficient
- C_{LG} - Glider lift coefficient
- C_{LT} - Tailplane lift coefficient
- C_m - Pitching moment coefficient
- C_{m_0} - Wing pitching moment coefficient
- C_T - Tangential force coefficient
- K_n - Static stability margin
- L - Total lift of glider
- L_T - Tailplane lift
- l - Distance of aerodynamic centre of tail aft of aerodynamic centre of glider without tail
- M - Pitching moment
- M_0 - Wing pitching moment about the a. c.

- N - Normal force
- n_G - Distance of glider c. g. below mean aerodynamic chord measured perpendicularly.
- q - Dynamic pressure
- q_T - Dynamic pressure at tail
- S - Wing area
- S_T - Tailplane area
- T - Tangential force
- t_G - Distance of c. g. aft of a. c. of glider without tail measured parallel to the chord
- V - Tail volume coefficient $S_T \cdot l / S \cdot \bar{c}$
- W - Total weight of glider
- α - Incidence of wing
- α_T - Incidence of tailplane
- η_T - Tailplane setting relative to mean aerodynamic chord of wing
- ϵ - Mean angle of downwash at the tail
- η - Elevator deflection
- $\bar{\eta}$ - Elevator angle to trim
- φ - Angle of distortion of tail chord relative to wing chord
- φ_F - Angle of fuselage distortion
- φ_T - Angle of tailplane twist
- φ_W - Angle of wing twist
- $\bar{\varphi}_W$ - Mean angle of wing twist $\bar{\varphi}_W = \frac{\int_0^{\frac{b}{2}} \varphi_W |y| \cdot c/|y| \cdot dy}{S/2}$

3. Determination of stability margin taking account of finite stiffness.

This section gives the derivation of the stability-margin equation, allowing for the finite stiffness of the glider.

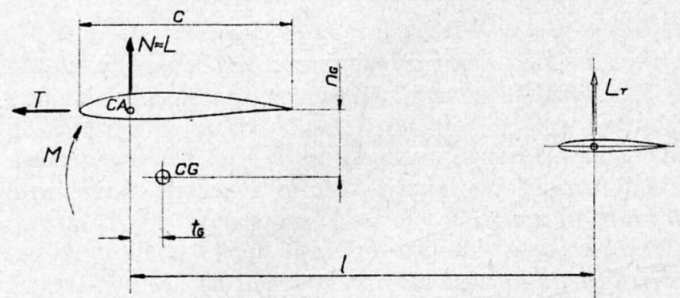


Fig. 1 - Equilibrium diagram

From fig. 1 it can be seen that the equilibrium condition for moments about the c. g. of the glider is:

$$M = M_0 + L \cdot t_G - T \cdot \eta_T - L_T (l - t_G) \quad [3.1]$$

Expanding the moments and forces in terms of aerodynamic coefficients yields:

$$C_m \cdot q \cdot S \cdot \bar{z} = C_{m0} \cdot q \cdot S \cdot \bar{z} + C_L \cdot q \cdot S \cdot t_G - C_T' \cdot q \cdot S \cdot n_G - C_{LT} \cdot q_T \cdot S_T (\ell - t_G) \quad /3.2/$$

By dividing the equation by $q \cdot S \cdot \bar{z}$, and assuming that $q_T/q \cong 1$ (which has been checked in flight tests) the relation for pitching moment coefficient is obtained:

$$C_m = C_{m0} + C_L \cdot \frac{t_G}{\bar{z}} - C_{LT} \cdot \frac{S_T}{S} \cdot \frac{\ell - t_G}{\bar{z}} - C_T \cdot \frac{n_G}{\bar{z}} \quad /3.3/$$

Differentiating Eq. /3.3/ with respect to lift coefficient gives:

$$\frac{\delta C_m}{\delta C_L} = \frac{t_G}{\bar{z}} - \frac{\delta C_{LT}}{\delta C_L} \cdot \frac{S_T}{S} \cdot \frac{\ell - t_G}{\bar{z}} - \frac{\delta C_T}{\delta C_L} \cdot \frac{n_G}{\bar{z}} \quad /3.4/$$

$$= \frac{t_G}{\bar{z}} \left[1 + \frac{\delta C_{LT}}{\delta C_L} \cdot \frac{S_T}{S} \right] - \frac{\delta C_{LT}}{\delta C_L} \cdot \frac{\ell}{\bar{z}} \cdot \frac{S_T}{S} - \frac{\delta C_T}{\delta C_L} \cdot \frac{n_G}{\bar{z}} \quad /3.5/$$

The total glider lift coefficient is:

$$C_{LG} = C_L + C_{LT} \cdot \frac{S_T}{S} \quad /3.6/$$

Differentiating Eq. /3.6/ with respect to C_L yields:

$$\frac{\delta C_{LG}}{\delta C_L} = 1 + \frac{\delta C_{LT}}{\delta C_L} \cdot \frac{S_T}{S} \quad /3.7/$$

hence:

$$\frac{\delta C_L}{\delta C_{LG}} = \frac{1}{1 + \frac{\delta C_{LT}}{\delta C_L} \cdot \frac{S_T}{S}} \quad /3.8/$$

Using the definition of stability margin:

$$K_n = \frac{\delta C_m}{\delta C_{LG}} = - \frac{\delta C_m}{\delta C_L} \cdot \frac{\delta C_L}{\delta C_{LG}} \quad /3.9/$$

Substituting Eq. /3.5/ and /3.8/ in /3.9/ gives:

$$K_n = - \frac{t_G}{\bar{z}} + \frac{\delta C_{LT}}{\delta C_L} \cdot \frac{\ell}{\bar{z}} \cdot \frac{S_T}{S} + \frac{\delta C_T}{\delta C_L} \cdot \frac{n_G}{\bar{z}} \cdot \frac{1}{1 + \frac{\delta C_{LT}}{\delta C_L} \cdot \frac{S_T}{S}} \quad /3.10/$$

The tailplane lift coefficient can be defined as:

$$C_{LT} = \frac{\delta C_{LT}}{\delta \alpha_T} \cdot \alpha_T \quad /3.11/$$

Fig. 2 shows the conditions at the tail.

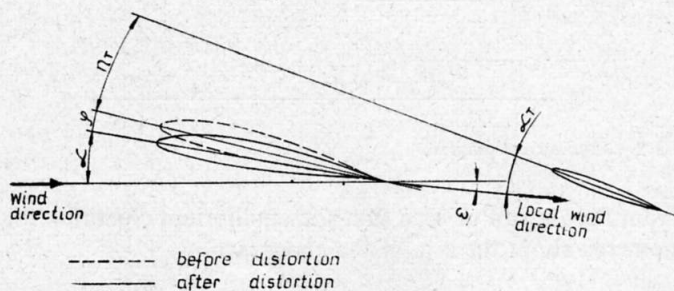


Fig. 2 - Method of allowing for distortion

The real tailplane incidence after allowing for distortion and downwash is:

$$\alpha_T = \alpha + \eta_T + \varphi - \epsilon \quad /3.12/$$

Substituting Eq. /3.12/ in /3.11/ gives:

$$C_{LT} = \frac{\delta C_{LT}}{\delta \alpha_T} \cdot (\alpha + \eta_T + \varphi - \epsilon) \quad /3.13/$$

In this equation $\eta_T = \text{const.}$ Differentiating with respect to C_L produces:

$$\frac{\delta C_{LT}}{\delta C_L} = \frac{\delta C_{LT}}{\delta \alpha_T} \left(\frac{\delta \alpha}{\delta C_L} + \frac{\delta \varphi}{\delta C_L} - \frac{\delta \epsilon}{\delta C_L} \right) \quad /3.14/$$

$$= a_1 \left(\frac{1}{a} + \frac{\delta \varphi}{\delta C_L} - \frac{\delta \epsilon}{\delta C_L} \right) \quad /3.15/$$

Substituting Eq. /3.15/ in /3.10/ leads to the final formula on the stick-fixed stability margin:

$$K_n = \frac{\delta C_m}{\delta C_{LG}} = - \frac{t_G}{\bar{z}} + \frac{a_1 \left[\frac{1}{a} + \frac{\delta \varphi}{\delta C_L} - \frac{\delta \epsilon}{\delta C_L} \right] \cdot \frac{\ell}{\bar{z}} \cdot \frac{S_T}{S} + \frac{\delta C_T}{\delta C_L} \cdot \frac{n_G}{\bar{z}}}{1 + a_1 \left[\frac{1}{a} + \frac{\delta \varphi}{\delta C_L} - \frac{\delta \epsilon}{\delta C_L} \right] \cdot \frac{S_T}{S}} \quad /3.16/$$

The above formula differs from the usual one for a rigid aircraft by the presence of the term $\delta \varphi / \delta C_L$ allowing for the influence of distortion.

The angle φ (see fig. 2) comprising the glider's distortion represents the change of the angle of the tailplane mean chord relative to the wing mean chord. This value is the sum of the distortions of the wing, fuselage, and tailplane, including their attachments:

$$\varphi = \bar{\varphi}_W + \varphi_F + \bar{\varphi}_T \quad /3.17/$$

What follows is based on the assumption that the angle is mainly influenced by the mean wing distortion $\bar{\varphi}_W$.

Note that the distortion of wing-fuselage attachment cannot be neglected.

Therefore:

$$\varphi \cong \bar{\varphi}_W$$

Knowing the wing torsional stiffness and the torque with respect to the speed the function $\bar{\varphi}_W = f(C_L)$ can be determined, which when differentiated with respect to C_L is to be substituted to Eq. /3.16/.

On fig. 3 there is shown for example the diagram of the above functions for the "Foka 4" glider, obtained from the distortions measurements given in fig. 8. The comparison of the two curves on fig. 3 shows that the function $\delta \bar{\varphi}_W / \delta C_L$ is more sloped than the $\bar{\varphi}_W$ curve. This results in the dominating influence of $\delta \bar{\varphi}_W / \delta C_L$ curve on the character of the stability margin.

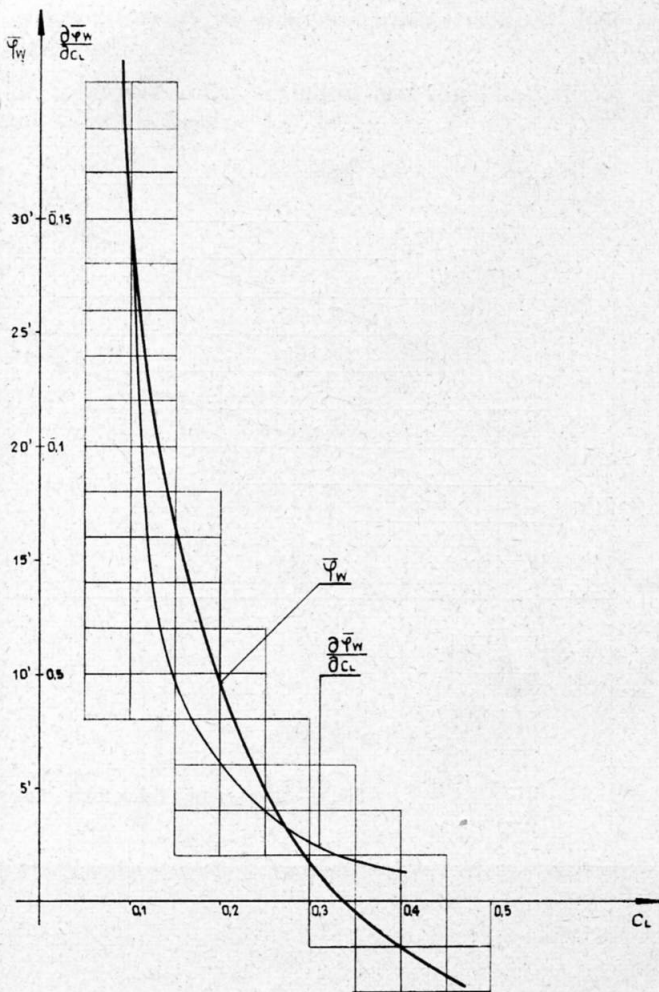


Fig. 3 - Distortion and its derivative as functions of lift coefficient, Foka

4. Determination of stick-fixed static stability margin from flight tests

The determination of stability margin is based on following assumptions:

- i. $\frac{W}{S} = \text{const.}$ - The c. g. variation is obtained by repositioning of ballast, the glider's weight being maintained constant,
- ii. $a_2 = \frac{dC_{L_T}}{d\eta} = \text{const.}$ and $\frac{d\alpha_T}{d\eta} = \text{const.}$

This is justified by the relatively small range of elevator deflection.

The stability margin can be defined as follows:

$$K_n = -\frac{dC_M}{dC_L} = -V \cdot a_2 \left(\frac{d\bar{\eta}}{dC_L} \right) \quad /4.1/$$

where:

$$V = \frac{s_T \cdot l}{s \cdot \bar{c}}$$

For determining the constant value $V \cdot a_2$ two equilibrium conditions related to the c. g. positions /1/ and /2/ are considered, C_L being constant.

For the first c. g. position:

$$C_{m1} = C_{m0} + C_L \cdot \frac{t_{G1}}{\bar{c}} - V (a_1 \cdot \alpha_T + a_2 \cdot \bar{\eta}_1) \quad /4.2/$$

and for the second:

$$C_{m2} = C_{m0} + C_L \cdot \frac{t_{G2}}{\bar{c}} - V (a_1 \cdot \alpha_T + a_2 \cdot \bar{\eta}_2) \quad /4.3/$$

For equilibrium:

$$C_{m1} = C_{m2} = 0$$

Subtracting Eq. /4.3/ from /4.2/ gives:

$$\frac{C_L}{\bar{c}} \cdot (t_{G1} - t_{G2}) - V a_2 (\bar{\eta}_1 - \bar{\eta}_2) = 0 \quad /4.4/$$

Rearrangement of /4.4/ produces:

$$V \cdot a_2 = \frac{C_L}{\bar{c}} \frac{(t_{G1} - t_{G2})}{(\bar{\eta}_1 - \bar{\eta}_2)} \quad /4.5/$$

Substituting Eq. /4.5/ in /4.1/ gives:

$$K_n = -\frac{C_L (t_{G1} - t_{G2})}{\bar{c} (\bar{\eta}_1 - \bar{\eta}_2)} \cdot \frac{d\bar{\eta}}{dC_L} \quad /4.6/$$

In the above formula the following terms appear:

- i. The difference $(t_{G1} - t_{G2})$ in per cent of M.A.C. is equal to the difference between the c. g. positions in two different flights.
- ii. $(\bar{\eta}_1 - \bar{\eta}_2)$ is the difference between the two angles of elevator deflection measured in flight at two c. g. positions at the same C_L .
- iii. $d\bar{\eta}/dC_L$ can be obtained by graphical differentiation of the function $\bar{\eta} = f(C_L)$ resulted from flight tests.

5. Flight tests results

5.1 Measurement of elevator deflection

The measurements of elevator deflection have been carried out for corresponding equivalent airspeeds (EAS) from the stall up to the placard speed at the foremost and aftmost c. g. positions. The gliders tested were fitted with a potentiometer connected by a lever system with the elevator. The logometrical indicator of that system was located in the cockpit. It has been proved that any deviation in trim tab setting produces errors, therefore the tab was locked in the neutral position on the elevator. The readings of deflection and airspeed indicator have been registered on a board tape recorder.

Fig. 4 et. seq. give the results for tests performed on SZD-24-4A "Foka 4" glider.

Fig. 4 shows the relation between elevator deflection and equivalent airspeed (EAS). Increase of speed corresponds to

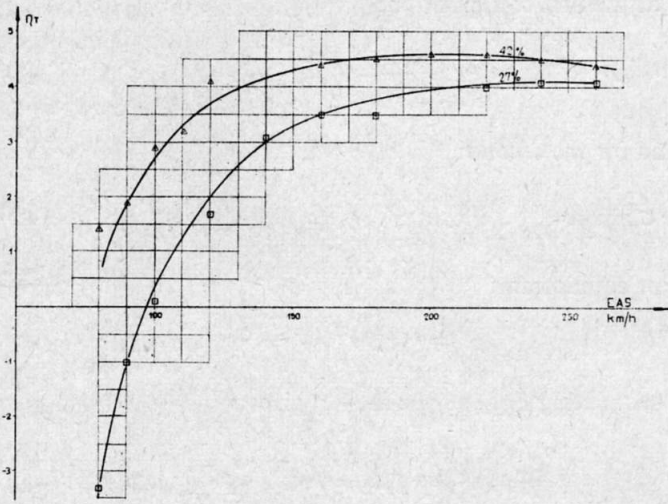


Fig. 4 – Elevator angle versus speed, Foka

decreasing elevator deflection increments, which become zero or even negative at some speeds. The absolute values of the increments are small over the significant range of speeds.

Fig. 5 shows the elevator deflection versus C_L . By graphical differentiation of this function and using Eq. /4.6/ the stability margins shown in fig. 6 were obtained.

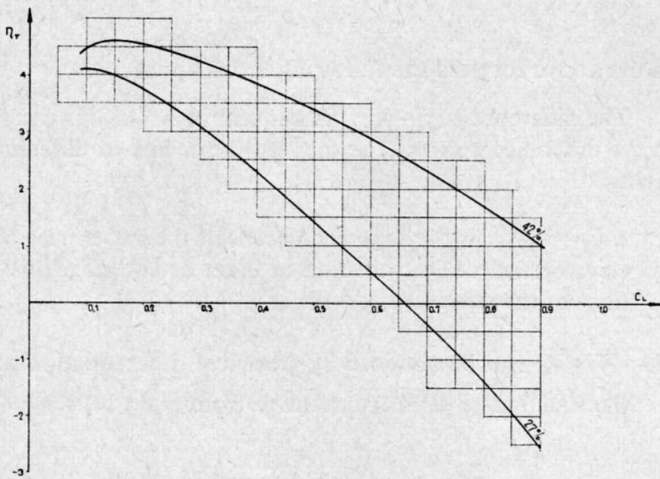


Fig. 5 – Elevator angle versus lift coefficient, Foka

5. 2 Measurement of wing twist

The wing twist measurement was based on a photographic method. Along the wing span there were situated four straight rods indicating the twist angles relative to a datum line in the plane of symmetry. The photographic equipment, electrically controlled, was mounted on the opposite wing. The twist angles were evaluated from enlarged photographs within ± 5 minutes.

The photograph fig. 7 shows the rods and the datum line on the fuselage. The tube of airspeed indicator can be seen on the wing tip.

Fig. 8 shows the results of the wing twist measurement for several speeds. The diagram indicates the relatively significant distortion between the first wing rod and the datum line, caused by the deformation of the wing-fuselage attachments.

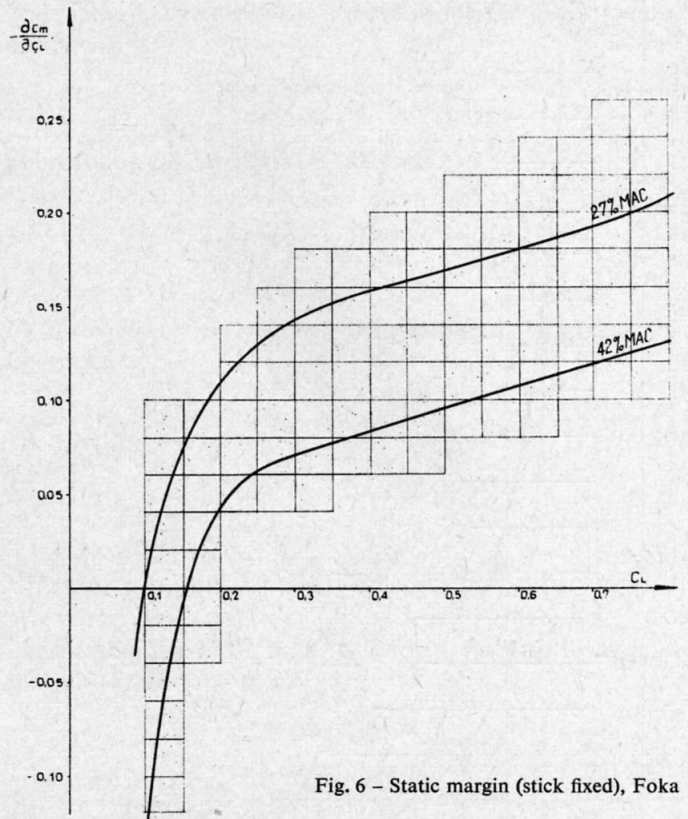


Fig. 6 – Static margin (stick fixed), Foka

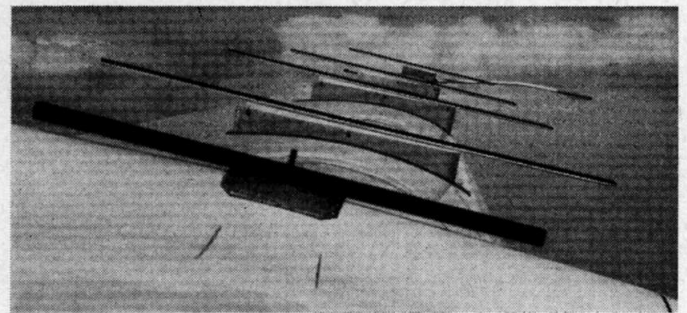


Fig. 7 – Measurement of wing twist distortion, Foka

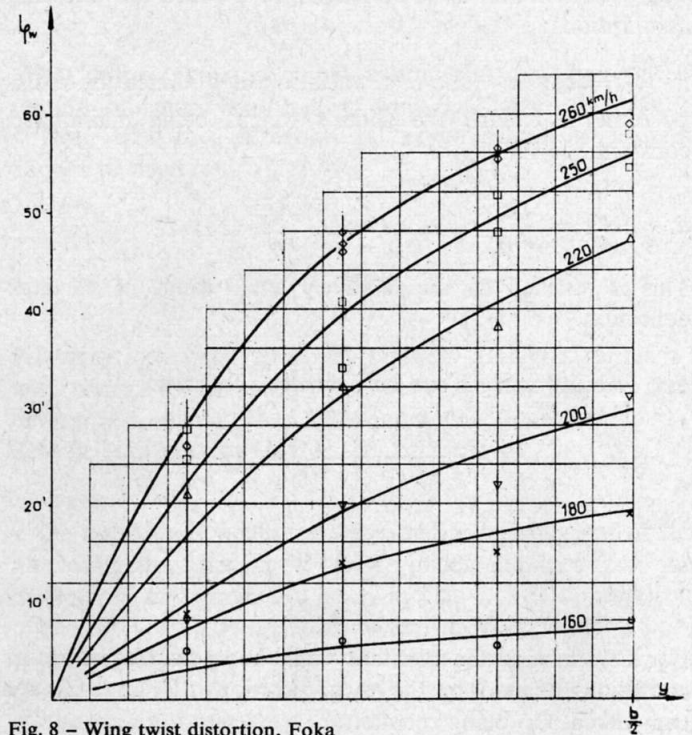


Fig. 8 – Wing twist distortion, Foka

6. Comparison of the analytical results with the flight test measurements

For comparison, the analytical and flight test results are both shown in fig. 9:

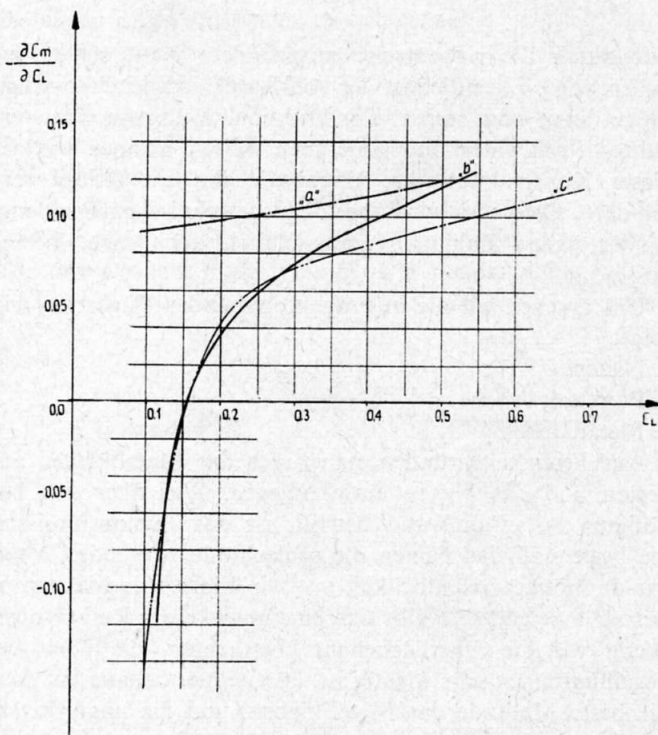


Fig. 9 – Estimated and measured static margin (stick fixed), Foka with C.G. at 42% M.A.C.

The particular curves on the diagram show the stability margin versus lift coefficient (for a given c. g. position):

- curve "a" – stability margin calculated neglecting the effects of distortion,
- curve "b" – results of calculations allowing for the effects of distortion,
- curve "c" – stability margin determined on the basis of elevator deflections measured in flight.

Zusammenfassung

Der Bericht behandelt die statische Stabilität mit festem Knüppel unter Berücksichtigung der Einflüsse endlicher Steifigkeit des Segelflugzeuges. Der passende Ausdruck für die Stabilitätsgrenzen wird abgeleitet; es wird davon ausgegangen, dass die elastische Verdrehung einfach als eine Änderung des Leitwerks-Einstellwinkels für einen gegebenen Auftriebsbeiwert abgeleitet werden kann (φ in Figur 2), Gleichung (3.16). Im allgemeinen besteht diese Änderung aus drei Teilen:

- a. der Verdrehung des Flügels
- b. der Biegung des Rumpfes
- c. der Verdrehung des Höhenleitwerks.

Zunächst ist die Ableitung der Stabilitätsgrenze aus den Flugmessungen des Höhenruderwinkels gezeigt, mit dem auf verschiedene Geschwindigkeiten bei zwei Schwerpunktlagen getrimmt wurde, Gleichung (4.6).

Mit dem Segelflugzeug Foka wurden beim S.Z.D. Messungen gemacht. Die Höhenruderwinkel für die Schwerpunktlagen bei 27 und 42% der mittleren aerodynamischen

An analysis of the curves shown in fig. 9 leads to following:

- i. In the higher C_L range the general character of the curves is similar and the differences of stability margin must be due to inaccuracies in the initial data (such as $\delta C_{LT}/\delta a_T$, $\delta C_L/\delta a$, effect of the fuselage on neutral point position and so on) used in the calculations.
- ii. At low C_L values the "a" curve neglecting the distortion differs distinctly from the curve "c" of the flight tests. The curve "b" based on calculations allowing for the distortion is similar to flight results.

Measurements as described above have been performed on gliders "Mucha Standard", "Zefir 2", "Blanik" and "Kobuz". The results obtained confirmed in all cases the need for allowing for distortion in stability calculations, if the true character of the stability margin is to be achieved.

7. Conclusions

1. The performed considerations show the essential influence of the stiffness of the glider on the character of the static stability margin with respect to C_L . To obtain true results this influence must be taken into account.
2. The negative static stability margin found in flight tests is not observable by a pilot using no special instruments and produces no dangerous behaviour of the glider.
3. From the safety point of view the stability characteristic found can be accepted provided that the reversal of elevator deflection is insufficient to be detected by the pilot and that the stick force gradient remains correct.

References

1. Ryszard Lewandowski
"Podstawowe pojecia z dziedziny statecznosci podluznej, sterownosci i zwrotnosci" – Technika Lotnicza 1/1950.
2. Wladyslaw Nowakowski
"Szybka metoda obliczania statecznosci statycznej platowca" – Technika Lotnicza 2/1951
3. Josef Hosek
"Aerodynamika vysokich rychlosti" - 1949.
4. A. W. Babister
"Aircraft Stability and Control" – Pergamon Press 1961.

Flügelteufe sind über der Geschwindigkeit in Figur 4 und über dem Auftriebsbeiwert in Figur 5 aufgetragen. Die Stabilitätsgrenzen werden in Figur 6 gezeigt. Die Verdrehung des Flügels und der Flügelrumpfbeschläge in Bezug auf den Rumpf wurde dadurch gemessen, dass man Messstäbe photographierte, die auf der Flügeloberseite und am Rumpf angebracht waren, wie es Figur 7 zeigt. Die Werte sind in Figur 8 aufgezeichnet.

Die Stabilitätsgrenze für 42% Schwerpunktlage verglichen mit den geschätzten Werten zeigt Figur 9. Die Kurven «a» und «b» sind Schätzungen, wobei «a» von der Annahme eines starren Segelflugzeuges ausgeht, und «b» die Wirkung der Flügelverdrehung und der Flügelrumpfbeschläge allein berücksichtigt und die Rumpfbiegung oder die Leitwerksverdrehung nicht betrachtet. Die Kurve «c» stellt das Flugergebnis dar; während es im Hochauftriebsbereich von der Schätzung ein wenig abweicht, ist die Übereinstimmung im Bereich kleiner Auftriebsbeiwerte sehr gut, weil hier die Verdrehungswirkungen gross sind.